Rotating saddle trap as Foucault's pendulum

Oleg N. Kirillov[a)]
Steklov Mathematical Institute, Russian Academy of Sciences, Moscow 119991, Russia

Mark Levi[b)]
Department of Mathematics, Pennsylvania State University, University Park, Pennsylvania 16802

(Received 30 January 2015; accepted 24 September 2015)

One of the many surprising results found in the mechanics of rotating systems is the stabilization of a particle in a rapidly rotating planar saddle potential. Besides the counterintuitive stabilization, an unexpected precessional motion is observed. In this note, we show that this precession is due to a Coriolis-like force caused by the rotation of the potential. To our knowledge, this is the first example where such a force arises in an inertial reference frame. We also propose a simple mechanical demonstration of this effect.
[http://dx.doi.org/10.1119/1.4933206]

I. INTRODUCTION

According to Earnshaw's theorem, an electrostatic potential cannot have stable equilibria (minima) because such potentials are harmonic functions. The theorem does not apply, however, if the potential depends on time. In fact, the 1989 Nobel Prize in physics was awarded to Paul[1] for his invention of a trap for suspending charged particles in an oscillating electric field. Paul's idea was to stabilize the saddle by "vibrating" the electrostatic field, by analogy with the so–called Stephenson–Kapitsa pendulum,[2–7] in which the upside–down equilibrium is stabilized by vibration of the pivot. Instead of vibration, the saddle can also be stabilized by rotation of the potential (in two dimensions), as has been known for nearly a century. As early as 1918, Brouwer (1881–1966), one of the authors of the fixed point theorem in topology, considered stability of a heavy particle on a rotating slippery surface.[8–10]

Brouwer derived the equations of motion for this system in Refs. 8 and 9; the derivation took over 3 pages. He then linearized the equations by discarding quadratic and higher order terms in position and velocity. The resulting *linearized* equations in the *stationary* frame are[11–13]

$$\ddot{x} + x\cos 2\omega t + y\sin 2\omega t = 0, \tag{1}$$

$$\ddot{y} + x\sin 2\omega t - y\cos 2\omega t = 0, \tag{2}$$

where $\omega = \Omega/\Omega_0$ is a dimensionless angular velocity, the dimensional angular velocity Ω scaled by $\Omega_0 = \sqrt{g/r}$, and where t is a dimensionless time, related to the dimensional time $\hat{t}$ by $t = \omega\hat{t}$.[14]

Equations (1) and (2) can be written in vector form as

$$\ddot{\mathbf{x}} + \mathsf{S}(\omega t)\mathbf{x} = \mathbf{0}, \tag{3}$$

where

$$\mathsf{S}(\omega t) = \begin{pmatrix} \cos 2\omega t & \sin 2\omega t \\ \sin 2\omega t & -\cos 2\omega t \end{pmatrix}. \tag{4}$$

We note that these equations are written in the stationary frame, whereas Brouwer actually derived the corresponding equations in a frame rotating with the saddle.[8–10] Equations (1) and (2), or, equivalently, Eq. (3), when written in the rotating frame, acquire Coriolis and centrifugal forces, but lose time-dependence because the saddle appears stationary in the co-rotating frame; the equivalence of the autonomous linear equations of Brouwer and the time-periodic Eqs. (1) and (2) is well-known (see, e.g., Refs. 12 and 13).

A particle in a rotating potential. Equations (1) and (2) also arise in a different context; they govern the motion of a unit mass *in the plane* under the influence of a potential force given by the rotating saddle potential—the potential whose graph is obtained by rotating the graph of $z = (1/2)(x^2 - y^2)$ around the z-axis with angular velocity ω. This *planar* problem is related to, but different from that depicted in Fig. 1. Physically, such a problem arises, for instance, in the motion of a charged particle in a rotating electrostatic potential, as discussed in Ref. 15.

Brouwer's particle vs a particle in a rotating potential. If the graph of the saddle surface in Fig. 1 is given by a function $z = f(x, y, t)$, then the potential energy of the unit point mass on the surface is $U(x, y, t) = gf(x, y, t)$. If we now take the same function U as the potential energy of a particle that lives in the plane, we get a problem related to Brouwer's, but not an equivalent one. To mention one aspect of the difference between the two problems, note that, unlike a particle in the plane, a particle on the surface feels centrifugal velocity-dependent forces due to the constraint to the surface. For the motions near the equilibrium, these forces are

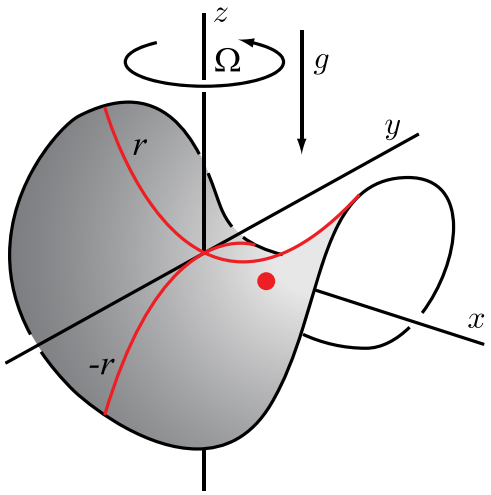

Fig. 1. A unit mass on a saddle (Refs. 8–10).

quadratically small (as was shown by Brouwer and as we will explain shortly), and they disappear upon linearization. And if U itself happens to be quadratic in x and y (as it is in our case), then the equations for the two problems are the same.

We would like to add a general remark on the difference between two similar problems: a particle on a surface $z = f(x, y, t)$ in a constant gravitational field on the one hand, and a particle in the plane with a potential $U(x, y) = gf(x, y, t)$ on the other. The two systems have the same potential energy; this is the similarity. But here is the difference: the kinetic energy for the particle in the planar potential is simply $K_{\text{plane}} = (1/2)(\dot{x}^2 + \dot{y}^2)$, while for the particle on a surface the kinetic energy is much more complicated:

$$2K_{\text{surface}} = (1 + f_x^2)\dot{x}^2 + 2f_x f_y \dot{x}\dot{y} + (1 + f_y^2)\dot{y}^2. \tag{5}$$

Here, f_x and f_y denote partial derivatives of the height function f. However, because $f_x = f_y = 0$ at equilibrium, these derivatives are small nearby and therefore $K_{\text{surface}} \approx K_{\text{plane}}$ near an equilibrium. Thus, the near-equilibrium motions of the two systems are quite similar.

Precessional motion in the rotating saddle trap. It has been known since Brouwer that the motion of a particle on a saddle is stabilized for all sufficiently high ω (Refs. 16 and 17). An illustration of a similar (but not equivalent) counterintuitive effect consists of a ball placed on a saddle surface rotating around the vertical axis and being in stable equilibrium at the saddle point.[18] We note, however, that the rolling ball on a surface is a non-holonomic system, entirely different from a particle sliding on a surface.[19,20]

The particle trapped in the rotating saddle exhibits a prograde precession in the laboratory frame, as illustrated in Fig. 2. This means that the particle moves along an elongated trajectory that in itself slowly rotates in the laboratory frame with the angular velocity ω_p in the same sense as the saddle. Up to now, this precession has been explained by analyzing explicit solutions of the linearized equations,[11,15,18] leaving the underlying cause of this precession somewhat mysterious.

II. DERIVING THE EQUATIONS OF MOTION

The motion of a unit point mass $\mathbf{x} = (x, y)$ in any time-dependent potential $U(x, y, t)$ is given by

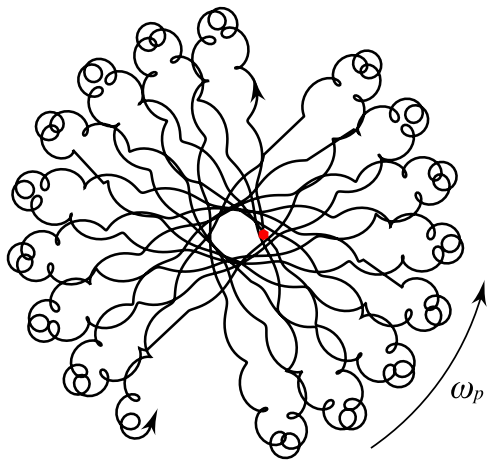

Fig. 2. Prograde precession of a particle on a rotating saddle in the non-rotating frame for large angular velocity ω calculated according to Eqs. (1) and (2). In this illustration, $\omega = 20/9 \approx 2.2$ (which is not even that large).

$$\ddot{\mathbf{x}} = -\nabla U(\mathbf{x}, t), \tag{6}$$

the gradient here is taken with respect to the (x, y) coordinates. The graph of our $U(\mathbf{x}, t)$ is obtained by rotating the graph of $U_0(x, y) = (1/2)(x^2 - y^2)$, and we must (i) find the expression for this rotated potential $U(\mathbf{x}, t)$, and (ii) compute ∇U (hopefully without having to use brute force).

The answer to (i) is simply

$$U(\mathbf{x}, t) = U_0(\mathsf{R}^{-1}\mathbf{x}), \tag{7}$$

where $\mathsf{R} = \mathsf{R}(\omega t)$ denotes a rotation through the angle ωt around the origin (counterclockwise if $t > 0$) and is given by the matrix (see Fig. 3)

$$\mathsf{R} = \mathsf{R}(\omega t) = \begin{pmatrix} \cos\omega t & -\sin\omega t \\ \sin\omega t & \cos\omega t \end{pmatrix}. \tag{8}$$

To answer (ii), we note that there are multiple ways of calculating ∇U. For example, we could write Eq. (7) in terms of x and y and then differentiate. A more elegant method is to write $U_0(\mathbf{x}) = (1/2)(x^2 - y^2)$ as the dot product

$$U_0(\mathbf{x}) = \frac{1}{2}(\rho\mathbf{x}, \mathbf{x}), \tag{9}$$

where $\rho = \text{diag}(1, -1)$ is a mirror reflection in the y-axis, and use this in Eq. (7) to get

$$\begin{aligned} U(\mathbf{x}, t) &= \frac{1}{2}\left(\rho\mathsf{R}^{-1}\mathbf{x}, \mathsf{R}^{-1}\mathbf{x}\right) = \frac{1}{2}\left(\mathsf{R}\rho\mathsf{R}^{-1}\mathbf{x}, \mathbf{x}\right) \\ &= \frac{1}{2}(\mathsf{S}\mathbf{x}, \mathbf{x}), \end{aligned} \tag{10}$$

where we have used the fact that R is an orthogonal matrix.

Now for any symmetric matrix S, one has $\nabla(\mathsf{S}\mathbf{x}, \mathbf{x}) = 2\mathsf{S}\mathbf{x}$, as one can see from the definition of the gradient,[21] and we conclude that

$$\nabla U(\mathbf{x}, t) = \mathsf{S}\mathbf{x}. \tag{11}$$

Thus, the equation of motion given by Eq. (6) turns into Eq. (3), as claimed.

A "spinning arrows" interpretation of a rotating saddle. Note that $\mathsf{S}(\omega t)$ is a composition of a reflection with respect to the x-axis and a counterclockwise rotation through angle $2\omega t$ [see Fig. 4(a)]. Therefore, for a *fixed* $\mathbf{x}$ and increasing t, the vector $\mathsf{S}(\omega t)\mathbf{x}$ rotates counterclockwise with angular velocity 2ω; this leads to the following geometrical

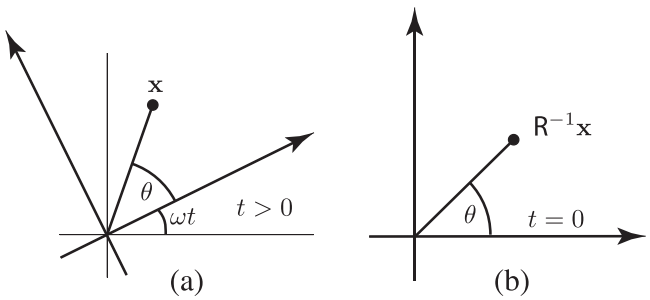

Fig. 3. Diagram providing an explanation for the rotation matrix in Eq. (7).

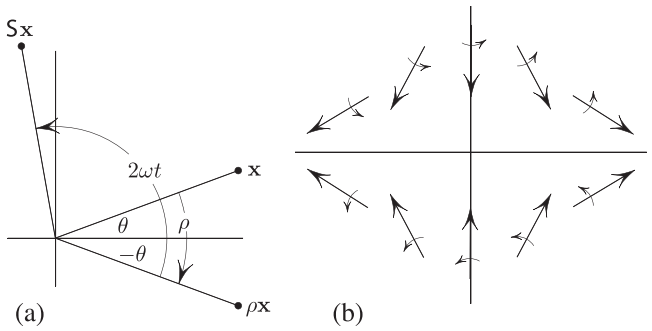

Fig. 4. (a) S is a reflection followed by a rotation. (b) Another interpretation of the rotating saddle: rotating the potential with angular velocity ω amounts to rotating each arrow of the vector field $\langle x, -y\rangle$ with angular velocity 2ω.

interpretation of the governing equations. The force field $-\mathsf{S}(\omega t)\mathbf{x}$ in Eq. (3) can be thought of in the following way. We start with the stationary saddle vector field $\langle x, -y\rangle$, and then rotate each arrow of this field counterclockwise with angular velocity 2ω [see Fig. 4(b)]. The result is our time-dependent vector field $-\nabla U(\mathbf{x}, t) = -\mathsf{S}(\omega t)\mathbf{x}$.

III. APPLICATIONS AND CONNECTIONS TO OTHER SYSTEMS

Before getting to the point of this note, we mention that Eqs. (1) and (2) arise in numerous applications across many seemingly unrelated branches of classical and modern physics.[12,16,18,22] Here is a partial list: they describe the stability of a mass mounted on a non-circular, weightless rotating shaft subject to a constant axial compression force;[17,23] in plasma physics they appear in the modeling of a stellatron—a high-current betatron with stellarator fields used for accelerating electron beams in helical quadrupole magnetic fields;[11,12,24] in quantum optics they originate in the theory of rotating radio-frequency ion traps;[15] in celestial mechanics they describe the linear stability of the triangular Lagrange libration points L_4 and L_5 in the restricted circular three-body problem;[25–27] and in atomic physics the stable Lagrange points were produced in the Schrödinger–Lorentz atomic electron problem by applying a circularly polarized microwave field rotating in synchrony with an electron wave packet in a Rydberg atom.[27] This last example has led to a first observation of a non-dispersing Bohr wave packet localized near the Lagrange point while circling the atomic nucleus indefinitely.[28] Recently, Eqs. (1) and (2) appeared in the study of confinement of massless Dirac particles (e.g., electrons in graphene).[29] And, interestingly, the stability of a rotating flow of a perfectly conducting ideal fluid in an azimuthal magnetic field possesses a mechanical analogy with the stability of Lagrange triangular equilibria and, consequently, with the gyroscopic stabilization on a rotating saddle.[30]

IV. THE RESULT: A "HODOGRAPH" TRANSFORMATION

The main point of this note is to show that the rapid rotation of the saddle gives rise to an unexpected Coriolis-like or magnetic-like force in the *laboratory* frame; it is this force that is responsible for prograde precession. To our knowledge, this is the first example where a Coriolis-like force arises in the inertial frame.

To state the result we assign to any motion $\mathbf{x} = \mathbf{x}(t)$ satisfying Eq. (3) its "guiding center," or "hodograph,"[31]

$$\mathbf{u} = \mathbf{x} - \frac{\varepsilon^2}{4}\mathsf{S}(\omega t)(\mathbf{x} - \varepsilon \mathsf{J}\dot{\mathbf{x}}), \tag{12}$$

where $\varepsilon = \omega^{-1}$ and where J is the counterclockwise rotation by $\pi/2$

$$\mathsf{J} = \begin{pmatrix} 0 & -1 \\ 1 & 0 \end{pmatrix}. \tag{13}$$

We discovered that for large ω (i.e., small ε), the guiding center has a very simple dynamics

$$\ddot{\mathbf{u}} - \frac{\varepsilon^3}{4}\mathsf{J}\dot{\mathbf{u}} + \frac{\varepsilon^2}{4}\mathbf{u} = O(\varepsilon^4); \tag{14}$$

that is, ignoring terms of $O(\varepsilon^4)$, $\mathbf{u}$ behaves as a particle with a Hookean restoring force $-(\varepsilon^2/4)\mathbf{u}$ and subject to the Coriolis- or magnetic-like force $(\varepsilon^3/4)\mathsf{J}\dot{\mathbf{u}}$. Figure 5 shows a typical trajectory of the truncated equation

$$\ddot{\mathbf{u}} - \frac{\varepsilon^3}{4}\mathsf{J}\dot{\mathbf{u}} + \frac{\varepsilon^2}{4}\mathbf{u} = 0, \tag{15}$$

which is in fact the motion of a Foucault pendulum. And just as with a Foucault pendulum,[32] the Coriolis-like term is responsible for prograde precession of $\mathbf{u}$ and thus of its "follower" $\mathbf{x}$.

Angular velocity of precession in Eq. (15) compared to earlier results. The angular velocity of precession of solutions of the Foucault-type Eq. (15) turns out to be $\omega_p = \varepsilon^3/8$. Indeed, writing the equation in the frame rotating with angular velocity ω_p gives rise to a Coriolis term and a centrifugal term, and the system in that frame becomes

$$\ddot{\mathbf{z}} + 2\omega_p \mathsf{J}\dot{\mathbf{z}} - \frac{\varepsilon^3}{4}\mathsf{J}\dot{\mathbf{z}} + \frac{\varepsilon^2}{4}\mathbf{z} + \omega_p^2\mathbf{z} = 0. \tag{16}$$

With the above value of ω_p, the second and the third terms cancel, and the resulting system

$$\ddot{\mathbf{z}} + \left(\frac{\varepsilon^2}{4} + \frac{\varepsilon^6}{64}\right)\mathbf{z} = 0 \tag{17}$$

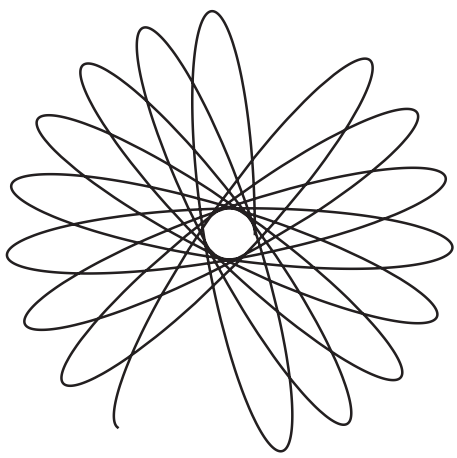

Fig. 5. The motion of the "guiding center," governed by Eq. (15), is the same as that of a Foucault pendulum. Here, $\varepsilon = 0.45$.

exhibits no precession at all (all solutions are simply ellipses). We conclude that $\varepsilon^3/8$ is indeed the angular velocity of precession of $\mathbf{u}$. This simple expression fits with the earlier results and also gives the precession speed for the near-equilibrium motions of Brouwer's particle, as we show next.

The equations of a rotating radio-frequency ion trap obtained in Hasegawa and Bollinger[15] reduce to our Eqs. (1) and (2) with $\varepsilon = \omega^{-1} = \sqrt{2q}$ after a re-scaling of time: $t = \tau\sqrt{2q}$. The time t is the dimensionless time appearing in Eqs. (1) and (2) while τ and q are, respectively, the dimensionless time and a dimensionless parameter of the trap in Hasegawa and Bollinger.[15] Calculating the angle of precession $\omega_p t$, we find

$$\omega_p t = \frac{\varepsilon^3}{8} t = \frac{\varepsilon^3}{8}\sqrt{2q}\tau = \frac{4q^2}{8}\tau = \frac{q^2}{2}\tau, \tag{18}$$

which yields the precession rate obtained by Hasegawa and Bollinger[15]

$$\omega_p^{HB} = \frac{q^2}{2}. \tag{19}$$

Similarly, the dimensional precession frequency of the particle in Fig. 1 is[12]

$$\Omega_p = \frac{g^2}{8r^2\Omega^3}. \tag{20}$$

A Coriolis-like force in the inertial frame. If $(\varepsilon^3/4)\mathsf{J}\dot{\mathbf{u}}$ were a true Coriolis force, it would have been due to the rotation of the reference frame with angular velocity $\varepsilon^3/8$, but our frame is inertial. Alternatively, one can think of $(\varepsilon^3/4)\mathsf{J}\dot{\mathbf{u}}$ as the Lorentz force exerted on a charged particle (of unit mass and of unit charge) in a constant magnetic field $B = \varepsilon^3/4$ perpendicular to the plane. Rapid rotation of the saddle gives rise to a virtual pseudo-magnetic force (cf. Refs. 33–35). As one implication, the asteroids in the vicinity of Lagrange triangular equilibria behave like charged particles in a weak magnetic field, from the inertial observer's point of view.

A numerical illustration. Figure 6 shows a numerical solution $\mathbf{x}$ alongside its "guiding center" $\mathbf{u}$. We note, as a side remark, that near the origin the solution follows the trajectory of the guiding center rather closely, reflecting the fact that oscillatory micromotion is small near the origin, as is clear from Eqs. (1) and (2).

We discovered the hodograph transformation in Eq. (12) via a somewhat lengthy normal form argument,[5,6] and which, due to its length, will be presented elsewhere. Nevertheless, once the transformation (12) has been produced, Eq. (14) can be verified directly by substituting Eq. (12) into Eq. (3); we omit the routine but slightly lengthy details, but give a geometrical view of this transformation.

A geometrical view of the hodograph transformation. Our result says, in effect, that the "jiggle" term

$$\frac{\varepsilon^2}{4}\mathsf{S}(\omega t)(\mathbf{x} - \varepsilon\mathsf{J}\dot{\mathbf{x}}) \tag{21}$$

in Eq. (12), when subtracted from $\mathbf{x}$, leaves a smooth motion.[36] Figure 7 gives a geometrical view of this term. It is still an open problem to find a simple heuristic explanation

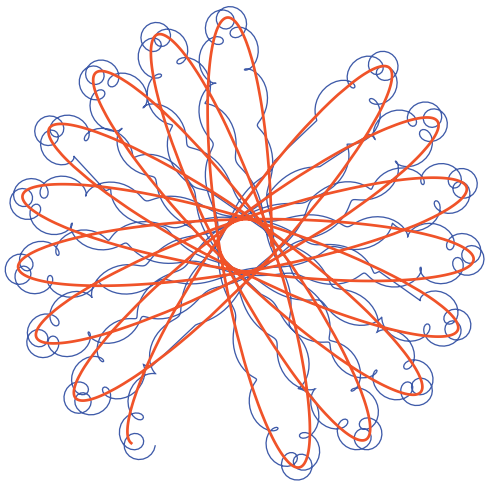

Fig. 6. A trajectory of the guiding center u governed by Eq. (15) (thick curve) tracking the corresponding trajectory $\mathbf{x}$ governed by Eq. (3) (thin curve). The view is in the inertial frame with $\varepsilon = 0.45$.

for the term $-\varepsilon\mathsf{J}\dot{\mathbf{x}}$ in Eq. (12). Finding a heuristic explanation of the "magnetic" term $(\varepsilon^3/4)\mathsf{J}\dot{\mathbf{u}}$ remains an open problem as well.

Validity of the truncation. Our result says that the fictitious particle $\mathbf{u}$, which shadows the solution $\mathbf{x}$, is subject to two forces: $-(\varepsilon^3/4)\dot{\mathbf{u}}$ and $-(\varepsilon^2/4)\mathbf{u}$, plus a smaller $O(\varepsilon^4)$ force. What is the cumulative effect of this smaller force? One can show, using standard results of perturbation theory, that neglecting the $O(\varepsilon^4)$ term leads to a deviation of less than $c_1\varepsilon^3$ over the time $|t| < c_2\varepsilon^{-2}$ for some constants c_1, c_2, for all ε sufficiently small. As it often happens with rigorous results, this one is overly pessimistic: computer simulations show that "sufficiently small" is actually not that small (for example, $\varepsilon = 0.45$ in Fig. 5). In fact, the reason for such an unexpectedly good agreement is the fact that the error on the right-hand side of Eq. (14) is actually $O(\varepsilon^6)$, two orders better than claimed, as follows from an explicit computation by Berry.[37] We do not focus on the analysis of higher powers of ε, because it would only add higher-order corrections to the coefficients on the left-hand side of Eq. (14), without affecting our main point (namely, that an unexpected Coriolis-like force appears).[38]

V. A PROPOSED EXPERIMENT

As mentioned in the introduction, a ball rolling on the rotating saddle surface[18] is *not* the right physical realization of the rotating saddle trap because (i) friction is very hard to

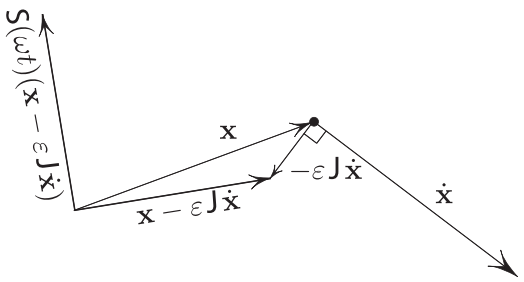

Fig. 7. A geometrical representation of the "jiggle" term $\mathsf{S}(\omega t)(\mathbf{x} - \varepsilon\mathsf{J}\dot{\mathbf{x}})$ (without the $\varepsilon^2/4$ factor) in the hodograph transformation. One should "read" the figure in the following order: $x \mapsto \dot{x} \mapsto -\varepsilon\mathsf{J}\dot{x} \mapsto x - \varepsilon\mathsf{J}\dot{x} \mapsto \mathsf{S}(x - \varepsilon\mathsf{J}\dot{x})$. A geometrical interpretation of S is shown in Fig. 4(a).

eliminate, and (ii) perhaps more importantly, because the rolling ball does not behave as a sliding particle. In fact, the rolling ball can be stable even *on top* of a sphere rotating around its vertical diameter.[20] Figure 8 illustrates a possible mechanical implementation of the rotating saddle trap (cf. Refs. 17 and 23). A light rod with a massive ball is essentially an inverted spherical pendulum; the sharpened end of the rod resting on the center of the platform acts as a ball joint with the horizontal plane. Two springs are attached to the rod,[39] and the height of the ball is adjustable, like in a metronome. If the ball is placed sufficiently low then the springs will stabilize the pendulum in the x-direction while the y-direction remains unstable [see Fig. 8(b) (Ref. 40)]; thus, the potential acquires a saddle shape

$$U_0(x,y) = \frac{1}{2}\left(ax^2 - by^2\right), \tag{22}$$

with a, $b>0$, ignoring higher powers of x, y. Here, $b = g/L$, where L is the distance from the ball to the sharpened end of the rod. In a moment, we suggest a simple way to adjust L to make the two curvatures equal ($a=b$) so that the linearized equations become

$$\ddot{\mathbf{x}} + b\,\mathsf{S}(\Omega t)\mathbf{x} = 0, \quad b = \frac{g}{L}, \tag{23}$$

which is a rescaled version of Eqs. (1) and (2). By rescaling the physical time t to the dimensionless time $\tau = \sqrt{a}t$, and introducing $\omega = \Omega/\sqrt{a}$, we transform the above equation into the dimensionless form of Eqs. (1) and (2) (after renaming τ back to t), which is stable if $\omega > 1$.[8,16,17]

Now $a = b = g/L$, where L is the distance from the mass to the ball joint, and using $a = \Omega^2/\omega^2$ then gives us the length

$$L = g\left(\frac{\omega}{\Omega}\right)^2. \tag{24}$$

The 78 rpm angular velocity of a vinyl record player corresponds to $\Omega \approx 8.2\,\mathrm{s}^{-1}$, and the value $\omega \approx 2.2$ referred to in Fig. 2 corresponds to a height $L \approx 71$ cm. How short can we make the pendulum without losing stability? The cutoff length is $L \approx 14$ cm, as follows from Eq. (24) and the fact that Eqs. (1) and (2) are stable if and only if $\omega > 1$. Incidentally, large L corresponds to large ω (for fixed rpm), which makes intuitive sense since a natural unit of time in our system is the period $2\pi\sqrt{L/g}$ of the oscillations along the stable axis of the stationary potential. For large L this period is long, and during one such cycle the rotating potential will spin many times, corresponding to large ω.

How to (easily) realize the saddle with equal principal curvatures. It may seem—as it did to us initially—that one needs to measure the stiffnesses of the springs, the various lengths in Fig. 8, the mass of the ball, and then use these to compute the value of L. Instead, here is a way to avoid all this work. Referring to Fig. 9, adjust the position of the massive ball along the rod to such critical height H_c as to make the ball neutrally stable in the x-direction: if the ball is too high (low), it will be unstable (stable) in the x-direction; a bisection method will quickly lead to a good approximation to H_c. Remarkably, the desired "equal curvatures" height of the ball is simply

$$L = \frac{H_c}{2}. \tag{25}$$

An explanation. The angle y satisfies the inverted pendulum equation $\ddot{y} - (g/L)\sin y = 0$, which for small angles is well approximated by

$$\ddot{y} - \frac{g}{L}y = 0. \tag{26}$$

Similarly, the linearized equation for the angle x is

$$\ddot{x} + \left(-\frac{g}{L} + \frac{k}{L^2}\right)x = 0; \tag{27}$$

L is not yet chosen, and k depends on the parameters of the system, but not on L.[41] Our goal is to find L such that the coefficients in the above equations are equal and opposite, which amounts to asking for L to satisfy $g/L = -g/L + k/L^2$, or

$$2Lg = k. \tag{28}$$

We now relate the unknown k to H_c. For a pendulum of length H_c, the angle x satisfies $\ddot{x} + (-g/H_c + k/H_c^2)x = 0$, with the coefficient $(-g/H_c + k/H_c^2) = 0$ since the equilibrium is neutral; this gives

$$k = gH_c. \tag{29}$$

Substituting $H_c = 2L$ into the last equation gives Eq. (28), precisely the condition for the equality of the coefficients in U.

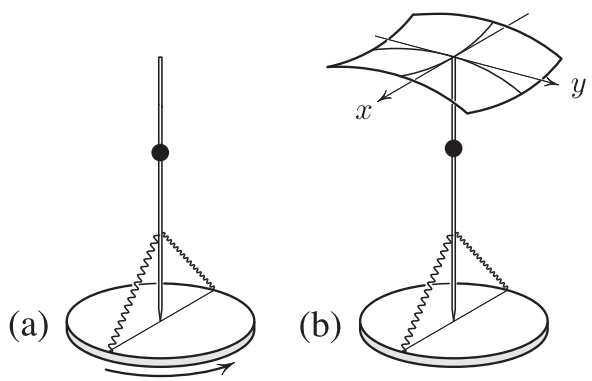

Fig. 8. A possible mechanical realization of the rotating saddle trap. Here, x and y are the angular variables of the inverted pendulum, and the graph of the potential energy in terms of the angular variables x, y is shown.

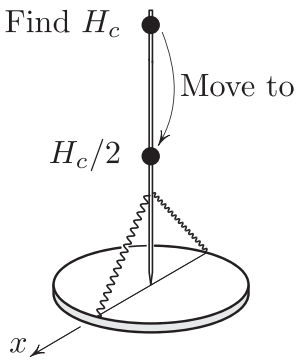

Fig. 9. How to find the length for which the curvatures of the saddle are equal and opposite: $U_{xx}(0,\,0) = -U_{yy}(0,\,0)$. Find, by trial and error, the height H_c at which the x-direction changes stability; the length of interest is then $H_c/2$.

VI. CONCLUSION

The existence of Trojan asteroids in a triangular Lagrange libration point on the orbit of Jupiter is a consequence of the basic fact that a particle can be trapped in the rotating saddle potential. In the case when the potential is symmetric, the trajectory of the trapped particle in the non-rotating frame exhibits a slow prograde precession. This somewhat mysterious precession discovered first in the context of accelerator physics and microwave ion traps has not been explained so far. We demonstrated that the rapid rotation of the saddle potential creates a weak Lorentz-like (or Coriolis-like) force, in addition to an effective stabilizing potential, all in the inertial frame. With the use of a new hodograph transformation and a method of normal form, we found a simplified equation for the guiding center of the trajectory that coincides with the equation of the Foucault's pendulum. In this sense, a particle trapped in the symmetric rotating saddle trap is, effectively, a Foucault's pendulum, but in the inertial frame. To demonstrate the phenomenon, we proposed a simple experiment with the inverted pendulum mounted on a turntable.

ACKNOWLEDGMENTS

Mark Levi gratefully acknowledges the support by the NSF grant DMS-0605878. Oleg Kirillov is thankful for partial support through the EU FP7 ERC grant ERC-2013-ADG-340561-INSTABILITIES.

[a]Electronic addresses: kirillov@mi.ras.ru and o.kirillov@hzdr.de; visiting DICAM, University of Trento, Trento I-38123, Italy.
[b]Electronic mail: levi@math.psu.edu

[1]W. Paul, "Electromagnetic traps for charged and neutral particles," Rev. Mod. Phys. **62**, 531–540 (1990).
[2]A. Stephenson, "On induced stability," Philos. Mag. **15**(86), 233–236 (1908).
[3]P. L. Kapitsa, "Pendulum with a vibrating suspension," Usp. Fiz. Nauk **44**, 7–15 (1951).
[4]L. D. Landau and E. M. Lifshitz, *Mechanics*, 1st ed. (Pergamon Press, Oxford, 1960), Vol. 1.
[5]M. Levi, "Geometry of Kapitsa's potentials," Nonlinearity **11**, 1365–1368 (1998).
[6]M. Levi, "Geometry and physics of averaging with applications," Physica D **132**, 150–164 (1999).
[7]V. I. Yudovich, "The dynamics of a particle on a smooth vibrating surface," J. Appl. Math. Mech. **62**(6), 893–900 (1998).
[8]L. E. J. Brouwer, "Beweging van een materieel punt op den bodem eener draaiende vaas onder den invloed der zwaartekracht," N. Arch. v. Wisk. **2**, 407–419 (1918).
[9]L. E. J. Brouwer, "The motion of a particle on the bottom of a rotating vessel under the influence of the gravitational force," in *Collected Works, II*, edited by H. Freudenthal (North-Holland, Amsterdam, 1975), pp. 665–686.
[10]O. Bottema, "Stability of equilibrium of a heavy particle on a rotating surface," Z. Angew. Math. Phys. **27**, 663–669 (1976).
[11]R. M. Pearce, "Strong focussing in a magnetic helical quadrupole channel," Nucl. Instrum. Methods **83**(1), 101–108 (1970).
[12]V. E. Shapiro, "The gyro force of high-frequency fields lost by the concept of effective potential," Phys. Lett. A **238**, 147–152 (1998).
[13]O. N. Kirillov, "Brouwer's problem on a heavy particle in a rotating vessel: Wave propagation, ion traps, and rotor dynamics," Phys. Lett. A **375**, 1653–1660 (2011).
[14]Note that Ω_0 is the frequency of small oscillations of the particle along the x-direction on the *non-rotating* saddle. Thus our dimensionless t measures time in the units of the period of the above mentioned oscillations.
[15]T. Hasegawa and J. J. Bollinger, "Rotating-radio-frequency ion traps," Phys. Rev. A **72**, 043403 (2005).
[16]O. N. Kirillov, *Nonconservative Stability Problems of Modern Physics*, De Gruyter Studies in Mathematical Physics Vol. 14 (De Gruyter, Berlin, Boston, 2013).
[17]K. Veselic, "On the stability of rotating systems," Z. Angew. Math. Mech. **75**, 325–328 (1995).
[18]R. I. Thompson, T. J. Harmon, and M. G. Ball, "The rotating-saddle trap: A mechanical analogy to RF-electric-quadrupole ion trapping?," Can. J. Phys. **80**, 1433–1448 (2002).
[19]J. I. Neimark and N. A. Fufaev, *Dynamics of Nonholonomic Systems*, Translations of Mathematical Monographs Vol. 33 (American Mathematical Society, Providence, RI, 2004).
[20]W. Weckesser, "A ball rolling on a freely spinning turntable," Am. J. Phys. **65**, 736–738 (1997).
[21]Indeed, the definition of the gradient of a function f states: $(\nabla f(\mathbf{x}), \mathbf{v}) \stackrel{\text{def}}{=} (d/ds)f(\mathbf{x}+s\mathbf{v})_{s=0}$ for all vectors $\mathbf{v}$. In our case, $f(\mathbf{x}) = (S\mathbf{x}, \mathbf{x})$ and $(d/ds)f(\mathbf{x}+s\mathbf{v})_{s=0} = (2S\mathbf{x}, \mathbf{v})$; comparing this with the left–hand side of the definition proves $\nabla(S\mathbf{x}, \mathbf{x}) = 2S\mathbf{x}$.
[22]O. N. Kirillov, "Exceptional and diabolical points in stability questions," Fortschr. Phys. Prog. Phys. **61**(2–3), 205–224 (2013).
[23]D. J. Inman, "A sufficient condition for the stability of conservative gyroscopic systems," Trans. ASME J. Appl. Mech. **55**, 895–898 (1988).
[24]C. W. Roberson, A. Mondelli, and D. Chernin, "High-current betatron with stellarator fields," Phys. Rev. Lett. **50**, 507–510 (1983).
[25]M. Gascheau, "Examen d'une classe d'equations differentielles et application à un cas particulier du probleme des trois corps," C. R. **16**, 393–394 (1843).
[26]K. T. Alfriend, "The stability of the triangular Lagrangian points for commensurability of order two," Celest. Mech. **1**(3–4), 351–359 (1970).
[27]I. Bialynicki-Birula, M. Kaliński, and J. H. Eberly, "Lagrange equilibrium points in celestial mechanics and nonspreading wave packets for strongly driven Rydberg electrons," Phys. Rev. Lett. **73**, 1777–1780 (1994).
[28]H. Maeda, J. H. Gurian, and T. F. Gallagher, "Nondispersing Bohr wave packets," Phys. Rev. Lett. **102**, 103001 (2009).
[29]J. Nilsson, "Trapping massless Dirac particles in a rotating saddle," Phys. Rev. Lett. **111**, 100403 (2013).
[30]G. I. Ogilvie and J. E. Pringle, "The non-axisymmetric instability of a cylindrical shear flow containing an azimuthal magnetic field," Mon. Not. R. Astron. Soc. **279**, 152–164 (1996).
[31]The conventional hodograph transformation involves the derivatives of the unknown function. Hamilton referred to the path of the tip of the velocity vector of an orbiting planet as the hodograph (the word is a combination of the Greek words for *path* and for *trace*, *or describe*.). Following Hamilton, in meteorology the hodograph is the trajectory of the tip of the velocity vector; in partial differential equations, Legendre's hodograph transformation involves partial derivatives. We refer to Eq. (12) as a hodograph transformation since $\mathbf{u}$ is a certain mixture of position and velocity.
[32]A. Khein and D. F. Nelson, "Hannay angle study of the Foucault pendulum in action-angle variables," Am. J. Phys. **61**(2), 170–174 (1993).
[33]M. V. Berry and J. M. Robbins, "Chaotic classical and half-classical adiabatic reactions: geometric magnetism and deterministic friction," Proc. R. Soc. A **442**, 659–672 (1993).
[34]M. V. Berry and P. Shukla, "High-order classical adiabatic reaction forces: Slow manifold for a spin model," J. Phys. A: Math. Theor. **43**, 045102 (2010).
[35]M. V. Berry and P. Shukla, "Slow manifold and Hannay angle for the spinning top," Eur. J. Phys. **32**, 115–127 (2011).
[36]As far as the powers up to ε^3 are concerned.
[37]M. V. Berry, personal communication (15 February 2015).
[38]According to M. Berry's computation (Ref. 37, see also Ref. 12) based on explicit solution of Eqs. (1) and (2), replacing the coefficient $\varepsilon^2/4$ in Eq. (15) by $\frac{\varepsilon^2}{4}\left(1+\frac{3}{16}\varepsilon^4+\frac{11}{128}\varepsilon^8+\cdots\right) = -\frac{(1-\sqrt{1-\varepsilon^2})(1-\sqrt{1+\varepsilon^2})}{\varepsilon^2}$, and replacing the coefficient $\varepsilon^3/4$ by $\frac{\varepsilon^3}{4}\left(1+\frac{5}{16}\varepsilon^4+\frac{21}{128}\varepsilon^8+\cdots\right) = \frac{2}{\varepsilon} - \frac{\sqrt{1-\varepsilon^2}+\sqrt{1+\varepsilon^2}}{\varepsilon}$ yields the equation for the exact guiding center (the expression for which is then given by Eq. (12), which includes higher order terms).
[39]Theoretically, we want to avoid transferring the rotation of the platform to the rotation of the rod around its long axis (thereby affecting its dynamics), and thus the attachment should, theoretically, be via some frictionless sleeve. In practice, however, this frictionless sleeve will hardly make a difference: the moment of inertia of the rod + ball around the long axis is negligible compared to the moment of inertia relative to a diameter of the platform, and thus the dynamics of the rod will be little affected by its axial rotation.
[40]Here, x and y are angular variables.
[41]Specifically, k depends on the springs' stiffness, on the angle they form with the diameter in Fig. 8, and on the ball's mass (to which it is inversely proportional). But an easier way to find k is to note that $k = gH_c$, as we show below.